Experimental and Theoretical Investigation of Drying of Green Peas in a Fluidized Bed Dryer of Inert Particles Assisted by Infrared Heat Source

Honarvar, Bijan
Chemical Engineering Department, Fars Science and Research Branch, Islamic Azad University, Fars, I.R. IRAN

Mowla, Dariush*+
Chemical Engineering, Department, Shiraz University, Shiraz, I.R. IRAN

Safekordi, Ali Akbar
Chemical Engineering Department, Sharif University of Technology, Tehran, I.R. IRAN

ABSTRACT: *Drying of green peas in a Fluidized Bed Dryer (FBD) with inert particle, heated by combined sources of hot air and InfraRed (IR) radiation, has been experimentally and theoretically studied. For this purpose, an experimental set up was constructed. This setup was composed of a cylindrical bed dryer containing some inert particles which are fluidized by hot air. Some infrared lamps were also placed around the bed for heating assistance. A sample of green pea was hung in the fluidized bed and its moisture content, surface and central temperature were measured with time. A mathematical model, based on the two layers concept of penetration and conduction was also proposed for this process. The results obtained by the proposed model were compared with the experimental data. Once the validity of the model was checked, it was used to investigate the effects of parameters such as inlet air velocity and temperature, drying sample size and the amount of inert particles on the rate of drying.*

KEY WORDS: *Fluidized bed, Inert particle, Infrared, Penetration layer, Conduction, Drying, Modeling, Green peas.*

INTRODUCTION

One of the most famous dehydration methods of food products is drying. The complication of the food drying process lies in the fact that the event should be carried out under a restricted temperature range since on one hand it is clear that at high temperatures the vapor pressure of water at the surface is high and water can evaporate rapidly with a high rate of drying, and on the other hand, high temperatures may change or damage the originality of the food stuff. So the challenge that remains in food industry, while reducing the moisture at an acceptable rate, is how can the temperature be keep low enough to avoid damaging the food stuff. This is why different

* *To whom correspondence should be addressed.*
+ *E-mail: dmowla@shirazu.ac.ir*
1021-9986/13/1/ 12/$/3.20

researchers have attempted to develop efficient ways of drying foods without damaging their originality.

Using a fluidized bed has the advantage of uniform drying at isothermal condition, however, the major disadvantage of this system is lower rate of drying (*Panda & Rao*, 1991 [1]; *Hovmand*, 1995[2]). Replacing the heat source of hot gas with IR radiation although increases the rate of drying, but it can create local hot spots and increase shrinkage since in this kind of system having a uniform distribution of temperature is impossible (*Zhou et al.*, 1998 [3]; *Hatamipour & Mowla*, 2003[4]; *Izadifar & Mowla*, 2002[5]). The combination of hot air and IR radiation in a FBD could be quite promising. This combined system will have the advantages of a high drying rate and uniform distribution of temperature and also giving a synergistic effect (*Hebbar et al.*, 2004[6]). The emission spectrums of infrared wave, used in the drying processes, are in the range of 0.1 to 100 micrometers (*Sandu*, 1986 [7]; *Souraki & Mowla*, 2008 [8]). In the case of opaque material in which the penetration depth can reach a few microns, the generated heat is transferred by conduction toward the center of the material which increases molecular vibration (*Sakai & Hanzawa*, 1994 [9]). Experimental studies on IR drying of various food products including vegetables have been reported by *Ginzburg*, 1969 [10]. The energy and quality aspects of drying of Barley in a combined IR and convection heat sources have been reported by *Afzal et al.*, 1999 [11].

The objective of this work was to investigate the drying of green peas in a FBD with inert particles using combined sources of hot air and IR experimentally and theoretically.

EXPERIMENTAL SECTION

Materials

In this work, which was designed to study the drying behavior of agro-food products, fresh green peas *(Pisum Sativum)* from Shiraz, situated in the south-west of Iran, were chosen as the drying product. Green peas were purchased from the same supplier to maximize the reproducibility of the results. Care was taken to select only green peas of spherical shape. The size of the pea grains was measured using a micrometer with an accuracy of 0.01 mm. Several measurements of the dimensions of the samples were made and only samples within a 5% tolerance of the average dimensions were used. Green peas were kept in a plastic container in a refrigerator at 4 °C for a minimum of 24 h in order to produce uniform initial moisture content throughout. After drying the samples in an oven at 105-110 °C for 24h, the average initial moisture content was found to be 77% on the wet basis. *Senadeera,* 2004 [12], reported initial moistures of 75-80% on the wet basis for this product.

Experimental work

A pilot scaled fluidized bed dryer with inert particles assisted by an infrared heating source, was set up for performing the drying experiments. The schematic diagram of the experimental apparatus is shown in Fig. 1 and a picture of the dryer section is shown in Fig. 2. The dryer was a cylindrical Pyrex column, 77.8 mm in diameter and 60cm in length, equipped with a perforated plate of 2mm perforation as an air distributor. The column was filled with glass beads, 3.0 mm in diameter as inert particles to increase mixing up and heat transfer coefficient, and also to improve the fluidity of the drying particles, and three infrared lamps, with 250 watt power each, were placed around the column to assist the heating. Drying air was supplied from a high pressure source and a pressure regulator was used to adjust the flow rate. Air was passed through a rotameter before being preheated by an electrical heater. A controller was used to regulate the temperature of the air; and the moisture content of the air was determined by an electronic humidity meter (HT-3015, Lutron, Taiwan). A Pea sample was hung in the fluidized bed filled with glass beads by means of a light string so that the sample could move freely with the inert particles. During the drying experiments, the weight of the green peas was determined at different times by means of an electronic balance with an accuracy of 0.001g (WAS 220/C/2, Radwag, Poland). The weighing procedure took no more than 10 seconds after removing the sample from the column. The surface, temperature as well as the central temperature of the sample, was measured by thermometer model (Type K/J/R/E/T + Pt 100 & Infrared Thermometer, Lutron, Taiwan) at different times of experimentation. At the beginning of each experiment, the velocity and the temperature of the drying air were adjusted to constant values. The operating conditions of each run are summarized in Table 1. The experimental set up was quite flexible in order to investigate the effects of different operating conditions on the rate of drying.

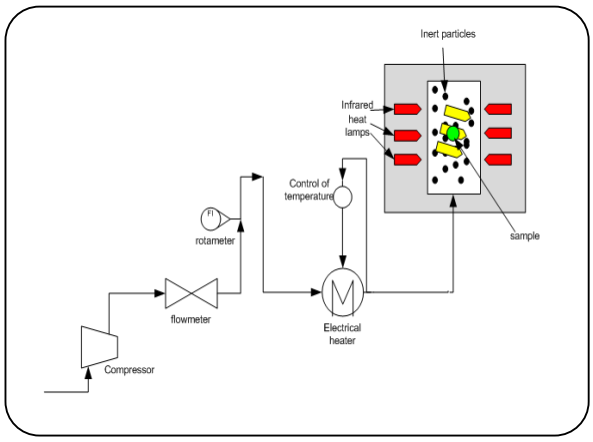

Fig. 1: Schematic diagram of the experimental apparatus.

Fig. 2: Fluidized Bed Dryer(FBD) assisted by infrared heating set up.

MATHEMATICAL MODELING

The mathematical model in this study includes one dimensional heat and mass transfer in the radial direction, and it was assumed that the absorptivity and infrared radiation by inert materials could be neglected.

Based on the theory of infrared irradiation, when infrared energy radiates from heaters it suddenly impinges upon the drying sample surface, directly penetrating into the grain approximately 1-2 mm under the surface, and is completely absorbed within this layer (*Ginzburg*, 1969[10]; *Nindo et al.*, 1995[13]; *Sandu*, 1986[7]). This layer is considered to be the zone affected by IR radiation and contains water vapors. Moisture in the form of liquid in the conduction zone is transferred to vapor at inter phase between the conduction zone and the penetration zone. The interior of the grain from a depth of 1-2 mm through to the center is called the conduction layer. In this layer IR radiation is ineffective and the moisture is in liquid form. This is one reason why the penetration zone is more porous than the conduction zone. During drying, heat is transferred by conduction from the surface of the penetration layer to the center zone. Moisture diffuses out to the surface, and the fluidizing gas, usually air, removes moisture from the surface to the void space of the dryer. In development of the mathematical model, it is assumed that heat reaches the surface of the drying sample grain by two mechanisms of convection and radiation, but diffuses into the interior of the sample only by conduction (*Jumah*, 2006 [14]). Based on this two-layer concept, energy and mass balances are predictably different for the two regions.

For the penetration layer the governing equations on a radial segment of the sample will be as follows:

$$\frac{\partial(\rho_p X_p)}{\partial t} = D_{eff}\left[\frac{\partial^2(\rho_p X_p)}{\partial r^2} + \frac{2}{r}\frac{\partial(\rho_p X_p)}{\partial r}\right] \quad (1)$$

$$\frac{\partial(\rho_p C_p T_p)}{\partial t} = K_P\left[\frac{\partial^2(T_p)}{\partial r^2} + \frac{2}{r}\frac{\partial(T_p)}{\partial r} + Q_r / K_p\right] \quad (2)$$

The solution of Eqs. ((1) and (2)) will be determined by using the following initial and boundary conditions:

At $t=0$ $0 \le r \le R_P$ $X_P=X_0$ (3)

At $t=0$ $0 \le r \le R_{sur}$ $T_P=T_0$ (4)

At $t>0$ $r=R_P$ $X_C = \frac{X_P \rho_{vap}}{\rho_{water}}$ (5)

At $t>0$ $r=R_s$ $-D_{eff}\frac{\partial(\rho_p X_p)}{\partial r} = K_m(y_e - y_\infty)$ (6)

At $t>0$ $r=R_p$ $T_C=T_p$ (7)

At $t>0$ $r\ R_S$ (8)

$$-K_P A_{Sur}\frac{\partial(T_P)}{\partial r} = hA_{Sur}(T_{Sur} - T\infty)$$

According to the theory of IR irradiation, IR energy from heaters suddenly impinges upon a grain surface, and directly penetrates into the grain, approximately 1 mm under the surface (*Ginzburg*, 1969[10]). Therefore, all of the IR energy is completely absorbed from the grain surface into the depth of 1mm, the so-called remove penetrating layer.

Table 1: The operating conditions for drying of green pea in a fluidized bed of inert particles assisted by infrared heat source.

Exp. #	Diameter of Samples,	Amount of Samples,	Air Velocity,	Inlet Air Temperature	Type of Inert	Amount of Inert,	Type of Infrared Experiment power	
No.	mm	gr	m/s	°C		gr		W
1	9.24	0.481	7	50	Glass	150	FBD	0
2	9.24	0.482	7	50	Glass	400	FBD	0
3	9.24	0.478	7	50	Glass	400	FBD	0
4	9.50	0.476	7	50	Glass	400	FBD with IR	600
5	9.05	0.491	7	50	Glass	400	FBD with IR	600
6	9.05	0.462	5	60	Glass	150	FBD with IR	600
7	9.14	0.457	5	50	Glass	150	FBD with IR	600
8	9.14	0.461	5	50	Glass	150	FBD with IR	600
9	9.12	0.457	5	40	Glass	150	FBD with IR	600
10	9.13	0.459	5	30	Glass	150	FBD with IR	600
11	9.13	0.460	5	60	Glass	150	FBD	0
12	9.14	0.464	5	60	Glass	150	FBD	0
13	9.14	0.467	5	50	Glass	150	FBD	0
14	9.14	0.472	5	40	Glass	150	FBD	0
15	9.13	0.463	5	40	Glass	150	FBD	0
16	9.14	0.462	5	35	Glass	150	FBD	0
17	9.14	0.461	2	50	Glass	400	FBD with IR	600
18	9.12	0.460	7	50	Glass	400	FBD with IR	600
19	9.14	0.472	2	50	Glass	400	FBD	0
20	9.14	0.462	7	50	Glass	400	FBD	0
21	9.14	0.465	7	50	Glass	400	FBD	0
22	8.61	0.417	3	40	Glass	400	FBD with IR	600
23	8.61	0.408	3	40	Glass	400	FBD with IR	500
24	9.46	0.417	3	40	Glass	400	FBD with IR	400
25	9.51	0.417	3	40	Glass	400	FBD	0

This layer is considered as location of the heat-convection. The interior of the grain, from the depth of 1 mm through to the grain is called the conduction layer in which heat is transferred by conduction. Conversely moisture inside the green pea grain is transferred from the core to the grain surface. Besides, heat and moisture at the grain surface are lost in the air within the radiative chamber by natural convection.

And for the conduction layer, the conservation of mass and energy in a radial segment of the sample leads to the following equations:

$$\frac{\partial(\rho_p X_C)}{\partial t} = D_{eff}\left[\frac{\partial^2(\rho_p X_C)}{\partial r^2} + \frac{2}{r}\frac{\partial(\rho_p X_C)}{\partial r}\right] \quad (9)$$

$$\frac{\partial(\rho_p C_p T_C)}{\partial t} = K_P\left[\frac{\partial^2(T_C)}{\partial r^2} + \frac{2}{r}\frac{\partial(T_C)}{\partial r}\right] \quad (10)$$

The solution of Eqs. (9 and 10) will be determined by using the following initial and boundary conditions:

At $t=0$ $0 \le r \le R_P$ $X_C=X_0$ (11)

At $t=0$ $0 \le r \le R_{sur}$ $T_C=T_0$ (12)

At $t>0$ $r=0$ $\frac{\partial X_C}{\partial r} = 0$ (13)

At $t>0$ $r=R_P$ (14)

$$-D_{eff}A_C\frac{\partial(\rho_P X_C)}{\partial r} = 4\pi\rho_{vap}r^2\frac{\partial r}{\partial t} - D^{vap}A_C\frac{\partial(\rho_P X_P)}{\partial r}$$

At $t>0$ $r=0$ $\frac{\partial T_C}{\partial r} = 0$ (15)

At $t>0$ $r=R_p$ (16)

$$-K_C A_C\frac{\partial T_C}{\partial r} = -K_p A_P\frac{\partial T_P}{\partial r} + 4\pi r^2\rho_{water}h_{fg}\frac{\partial r}{\partial t}$$

The equilibrium moisture composition (X_e) in the inter phase at the surface of the drying particle is expressed by the equations of *Krokida et al.,* 2003 [15].

The equilibrium moisture control of air (Y_e) in the inter phase is expressed by *Strumillo & Kudra* ,1996 [16] and D^{vap} in the above equation is found by *Xiao Dong Chen*, 2006 [17].

In which y_e is the characteristics of balanced humidity in gas phase with drying materials in a shared part, so that the value of balanced humidity can be calculated by absolute humidity.

$$Y_e = \frac{M_{water}}{M_{air}}\frac{a_w(X,T)P_{sat}(T)}{P - a_w(X,T)P_{sat}(T)} \quad (17)$$

Put a_w water activity on the surface of the drying materials, calculated by some experimental relations of humidity absorption isotherm of different materials. a_w of the surface can be expressed as $RH_{equilibrium}/100$. For drying it is necessary to hold the inequality of $a_{w,\,surface}*100 > RH_{bulk\ air}$.

By calculating Y_e, the value of y_e can be calculated in the following equation:

$$y_e = \frac{Y_e}{0.622 + Y_e} \quad (18)$$

The value of the thermal conductivity of the wet material at the penetration area is obtained by the following equations:

$$Kp = 0.55X + 0.26(1-X) \quad (19)$$

and the value of k_c (thermal conductivity of conduction layer) is about 1840 kJ/kg°C, which was proposed by *Sir Earle* in 1997 [18].

The volume of average moisture content in drying materials is obtained by using the following equation:

$$X_{avg}(t) = \frac{4\pi}{V_p}\int_0^{R_P} r^2 X(r,t)dr \quad (20)$$

Q_r on the right side of Eq. (2) is the heat generated due to infrared radiation. To determine Q_r, it is assumed that infrared wave absorption obeys Lambert laws (*Weissteins*, 2005) [19], according to which the intensity of the adsorbed infrared energy decays exponentially as it moves from the surface toward the center of the sample. The amount of generated infrared heat can be calculated by the energy delivered to particle per unit volume of the penetration layer according to Lambert's law, which describes the conversion of infrared energy to thermal energy in a semi infinite free body as follows:

$$Q_r = (Q_{Abs}\exp[-k(R_P - r)])/(\frac{4\pi}{3}(R_S - R_p)^3)) \quad (21)$$

Q_{Abs} is the initial radiant heat absorbed by the sample on the surface, k is the extinction coefficient (m^{-1}) and $d_{pen}=1/K$ is the penetration depth (m) (*Jun & Irudayaraj*, 2003) [20].

The value of K, related to extinction coefficient, is researched experimentally by means of the thermocouple PT-100 in the laboratory.

The penetration depth was calculated by measuring the temperature changes in different layers of material diameter based on the following relation:

$$K = \frac{1}{d_p} \tag{22}$$

This was obtained at the range of 0.7 to 1 mm. In this study it is considered as K=1150 with penetration depth of 0.87mm.

To calculate Q_r from Eq. 19 it is necessary to find Q_{Abs}, which is the quantity of infrared energy delivered to the particle by the IR heater. For this purpose the following equation is used:

$$Q_{Abs} = \frac{\sigma(T_e^4 - T_{sur}^4)}{\frac{1-\varepsilon_{IR}}{\varepsilon_{IR} A_{IR}} + \frac{1}{F_{gp-IR} A_{IR}} + \frac{1-\varepsilon_{gp}}{\varepsilon_{gp} A_{gp}}} \tag{23}$$

The values of ε_{IR} and ε_{gp} are taken to be 0.9 the reported by *Anon*, 2004 [21] and 0.7 by *Arinze et al.*, 1984 [22] respectively.

The heat transfer coefficient can be obtained from the following relation (*Kunni & Levenspiel*, 1991 [23]).

$$Nu = 2 + 1.8 Re^{1/2} Pr^{1/3} \tag{24}$$

The lumped method was used to measure the value of the average heat transfer coefficient h_t. For this purpose a metal with high thermal conductivity, placed in the fluidized bed, was utilized to find the h_t value. In this regard, the fluidized bed dryer containing inert particles operates for about two hours to reach the thermal stable condition (constant temperature). An aluminum sphere was then introduced to the drying column. In each experiment, the temperature at the center of the aluminum sphere was measured at different time intervals in the presence of energy carrying particles (electromagnetic waves were not present). Experimental results showed that the presence of particles as energy carriers caused the solid temperature to reach the final temperature quickly. This analysis assumed negligible temperature gradient within the solid, thus heat transfer resistance was concentrated at the particle surface (*Ghisalberti & Kondjoyan*, 1999 [24]). With applying the initial condition ($T=T_0$ at t=0) and integrating the energy equation in the metal sample, the following equation is obtained:

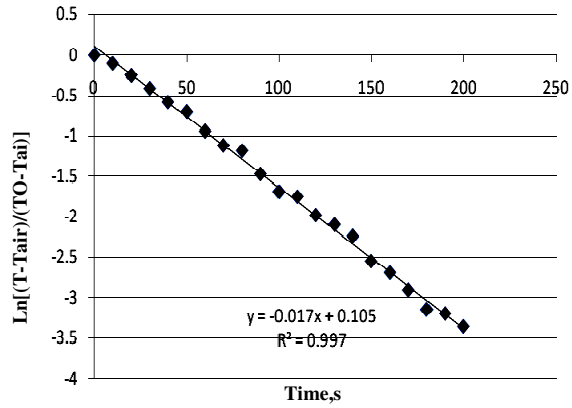

Fig. 3: Plot of Ln(dimensionless temperature) vs time for determination of total heat transfer coefficient in a 2 cm diameter of aluminum sphere.

$$\frac{T - T_\infty}{T_0 - T_\infty} = \exp\left[-\frac{h_t A}{\rho C_P V} t\right] \tag{25}$$

Temperature-time data is plotted as $Ln\left(T - T\infty / T_0 - T\infty\right)$ versus time as shown in Fig. 3. The slope of the line was used for calculating the overall heat transfer coefficient. The experiment was repeated 3 times for different sizes of aluminum spheres. The average heat transfer coefficient for the sphere with a diameter of 20 mm in the fluidized bed with an air temperature of 50 ˚C was about 137 ±4.5 W/m^2K. It is noteworthy that due to the mixing and turbulence in the fluidized beds, the heat transfer coefficient between the floating sample and the bed was in the order of (100-400) W/m^2K (*Botterill*, 1975 [25]).

The convective mass transfer coefficient K_m is obtained from the heat and mass transfer analogy as (*Incorpera & Dewitt*, 1996 [26]):

$$\frac{h_t}{K_m} = \rho_a C_{pa} Le^{\frac{2}{3}} \tag{26}$$

The following relation is use to calculate the Lewis Number:

$$Le = \frac{Sc}{Pr} = \frac{\mu}{\rho D_{AB}} \cdot \frac{\kappa}{\mu C_p} = \frac{\alpha}{D_{AB}} \tag{27}$$

The value of Prandtl Number for temperatures ranging 40 °C to 80 °C is 0.788. The Schmidt Number is about 0.66, and the value of Lewis Number based on the mentioned relation is 0.9

The physical properties of air to be used in the above equations are obtained from the work of *Pakowsk et al.*, 1991 [27]. The volume average particle temperature is obtained using the following equations:

$$T(t) = \frac{4\pi}{V_p}\int_0^{R_p} r^2 T(r,t)dr \quad (28)$$

The correlation obtained by *Honarvar et al.*, 2009, 2010, [28, 29] was applied for the calculation of the moisture effective diffusivity.

$$D_{eff} = 1.3*10^{-5}\exp\left(\frac{-3120}{T_a}\right)\exp\left[(-0.00812T_a + 2.7)X\right] \quad (29)$$

Applying the finite difference method to the Eqs. (1 and 2) and (9 and 10) provided a tri-diagonal matrix, suitable for using the implicit finite difference method.

Solution of the model

Partial differential Eqs. (1, 2, 9 and 10) with the internal heat generation term specified by Eq. (21), and the initial and boundary conditions specified in Eqs. (3 to 8) and (11 to 16), were solved by the semi explicit-implicit form of the Crank-Nicolson scheme. A sphere was divided into 10 concentric shells of equal thickness and 3500 intervals for time. Finite difference approximation was formulated using second order central differentiation in space, and a first order difference in time. The resulting system of algebraic equations was solved using a MATLAB program, written for this purpose.

RESULTS AND DISCUSSION

Fig. 4 shows how the moisture content of green peas is reduced from the initial value to the final values for both systems of FBD and FBD with IR during a forty-minute drying process. As is observed from this figure, using IR together with hot gas enhances the drying rate during both types of experiments. It should also be mentioned that the initial surface moisture of the samples was the same during all experiments, and since the initial surface moisture was small, the drying process started in a falling rate regime An interesting observation from the experimental data is that, at the beginning of drying, since the moisture content is high, the presence of IR has little effect, while by increasing the drying time, as the moisture content is reduced and mass transfer becomes difficult, the presence of IR becomes more noticeable. Another interesting point about the experimental data is that, although for both cases the initial moisture content of the sample is the same, at the end of the drying period a lower fraction of moisture remains in FBD with IR in comparison to the FBD. This is because, as explained before, there was no intention of lowering the moisture content beyond a value in which the shrinkage becomes significant. As one can see from this Fig. 4, X (kg of moisture to kg of dry solid) was never allowed to get below one, otherwise, if there is enough time for drying and no worry about shrinkage, these two curves should converge to the same values of the moisture content. It should be remembered that since shrinkage beyond a limited value would completely change the geometry of the sample, the physical situation will differ and the above discussion might not hold firm. It should be mentioned that ultimately the water content of the sample can only reach the equilibrium value of water vapor in drying air and can never be zero. Due to the lack of other experimental data for the combined mechanism of heat transfer in the fluidized bed, no comparison of the result was possible, but for the case without infrared, the results of this work were in agreement with the work of *Hatamipour & Mowla,* 2003 [4]. Fig. 4 also shows the results obtained from the mathematical model for both systems, and as can be seen, good agreement exists between the experimental and model results.

Fig. 5 shows the results obtained experimentally and theoretically for variation of the surface temperature of the drying samples in both systems. In fact, the results in Fig. 5 reconfirm the results which are shown in Fig. 4. As can be seen from Fig. 5, the surface temperature of the sample is much higher when the combined heat sources of hot gas and IR are used in comparison with FBD. This high surface temperature translates to a high concentration of moisture in the surface, since vapor pressure increases with temperature. Comparing the identical sample with the same initial center moisture content, the sample having a higher surface temperature will have a higher driving force for mass transfer between the surface and gas stream. At first glance it might seen that since the controlling step of mass transfer is diffusion within the solid, inter phase mass transfer should play no role, but in fact, as mentioned, in the penetration layer the moisture

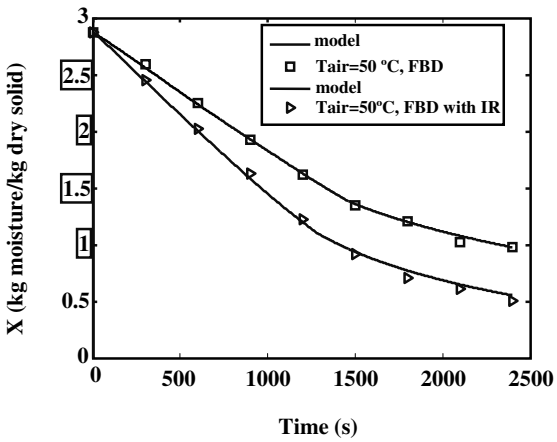

Fig. 4: Comparison between experimental and predicted average moisture contents of green peas sample in both system FBD & FBD+IR (T=50 °C, V=2m/s, Mip =400g, dia=9mm).

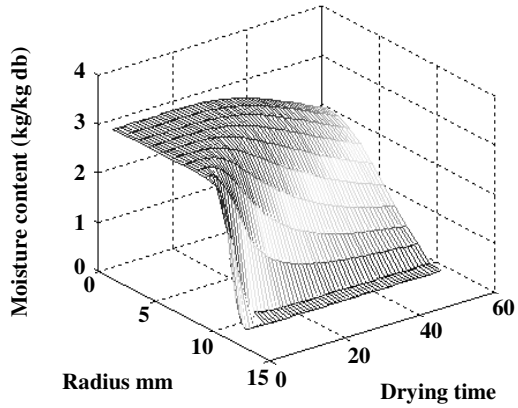

Fig. 6: Development of the moisture distribution in green peas sample during drying in fluidized bed dryer assisted by infrared heat source (T=50 °C, M_{ip} =400g, dia=10mm, Power=600W, V = 3m/s).

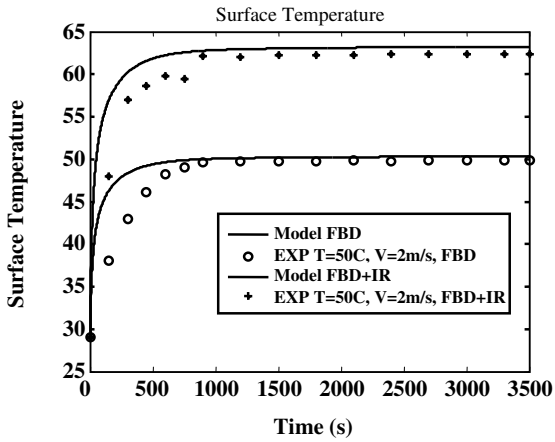

Fig. 5: Comparison between experimental and predicted surface temperature of green peas sample in both systems, FBD & FBD+IR (T=50 °C, V=2m/s, Mip =400g, dia=9mm).

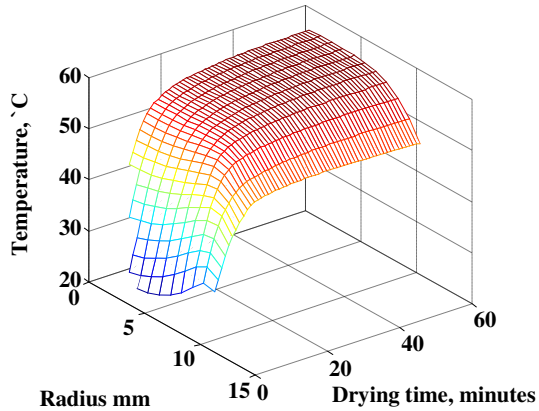

Fig. 7: Development of the temperature in green peas sample during drying in fluidized bed dryer assisted by infrared heat source (T=50 °C, M_{ip} =400g, dia=10mm, Power=600W, V = 3m/s).

in the vapor phase and moving from the inside toward the surface by diffusion. Without a doubt, when the surface temperature is high it is clear that in the whole penetration layer the temperature gets higher, and since diffusion increases with temperature, moisture reaches the surface faster and easier. This creates a higher driving force between the surface and the gas stream. When with the aid of IR the heat source is increased, not only the surface temperature increases, but the temperature in the penetration layers should also be expected to increase. So relatively speaking, when IR is used, more vapors are to be moved out from the solid. The results of this figure show that in both systems the model over predicts the surface temperature. One reason for is that measuring the temperature on the surface is a very difficult task and the sensors used for measurement of the sample temperature are in fact located in the outer layer of the penetration layer which becomes colder due to the flowing air. Because the system is considered as an adiabatic system for the calculation of transfer phenomena, some theoretical relations and experimental data are used, so the resulted difference is related to heat losses.

In Figs. 6 and 7 the variations of moisture content and temperature inside the drying sample are shown as a function of time and location. Fig. 7 shows that the temperature drops at the surface slightly in the first

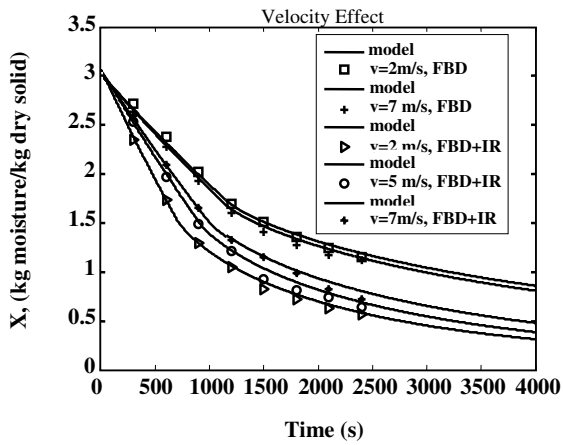

Fig. 8: Experimental and predicted average moisture contents of green peas in two different drying air velocities of 2 and 7 m/s in both systems (FBD & FBD+IR).

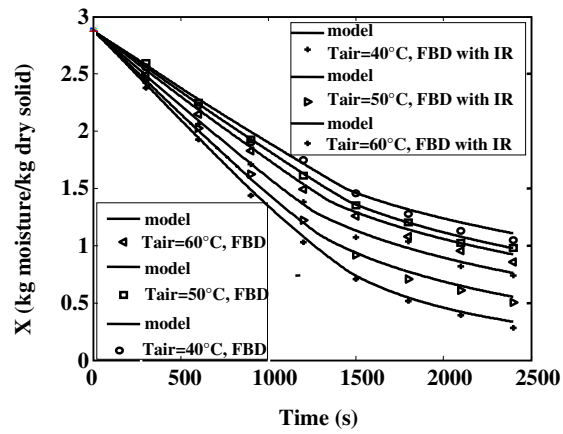

Fig. 9: Experimental and predicted average moisture contents of green peas in three different drying air temperatures of 40, 50, 60 °C in both systems (FBD & FBD+IR).

second of drying because of evaporative cooling during the surface evaporation. The temperature rises slowly in the beginning stages of drying since infrared heating is more efficient in a larger moisture content of green peas. During this period the absorbed infrared energy is higher than the energy losses associated with the moisture evaporation and surface convective cooling.

The rate of drying of food products is affected by several factors and this complicates the drying processes more. Some of these complications are due to simultaneous heat and mass transfer, while other difficulties have roots in the limitations that exist in drying foodstuff. After gathering the experimental data and validating the proposed mathematical model, it was used to study the effects of different parameters on the rate of drying for these systems. Fig. 8 shows the variations of sample moisture content with flowing air velocity for two different systems of FBD and FBD with IR, while maintaining other all parameters constant. In this case the air velocity is changed from 2 m/s (minimum fluidizing velocity) to 7 m/s. For FBD with IR system, at low air velocity, the rate of water content loss was high as expected. This can be contributed to the fact that at higher air velocity more heat is lost due to forced convection, but for the other system (FBD) increasing air velocity shows varying results.

Fig. 9 shows theoretical drying characteristic curves for spherical particles of green peas for both systems of FBD and FBD+IR at different temperatures of drying air, ranging between 40 - 60 °C. As is expected, a rise in the air temperature leads to an increase in the drying rate. Fig. 10 shows the experimental and theoretical drying curves for spherical particles of green peas at different sample diameters. Analysis of the results shows that decreasing the diameters of the drying samples would increase the drying rate for the FBD with IR system faster than for the FBD alone.

Fig. 11 shows the drying curves for various amounts of inert materials presented to the bed. As can be seen from this figure, increasing the amount of inert material between 150 - 400 grams, a range which did not prevent the process of fluidization, slightly increases the rate of drying in both systems.

CONCLUSIONS

In this study we have successfully monitored the moisture content of green peas in a fluidized bed using hot gas and IR as the heat sources. A mathematical model for a fluidized bed dryer with inert particles assisted by infrared heating was developed as a series of equations for unsteady state drying of a single green pea particle. Simultaneous heat and mass transfer equations were solved using the finite difference scheme to predict the changes of temperature and moisture content of the sample. The model was developed under the assumption that two regions exist: a region of penetration which is dry and a region of conduction which is saturated. The model indicates that infrared radiation is more effective in reducing the moisture content of the green peas when they are wet rather than when they are dry. Good agreement between the experimental data and values

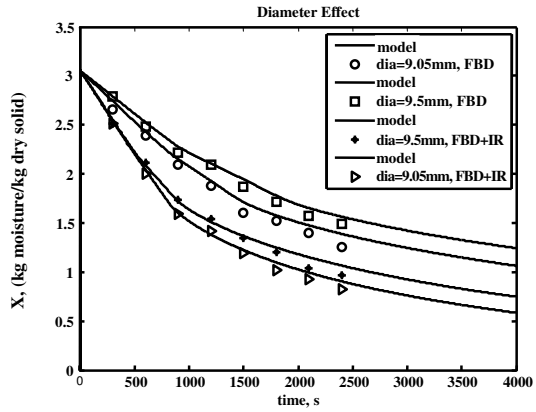

Fig. 10: Experimental and predicted average moisture contents of green peas in two different sample diameters of 9.05 and 9.5 mm in both systems (FBD & FBD+IR).

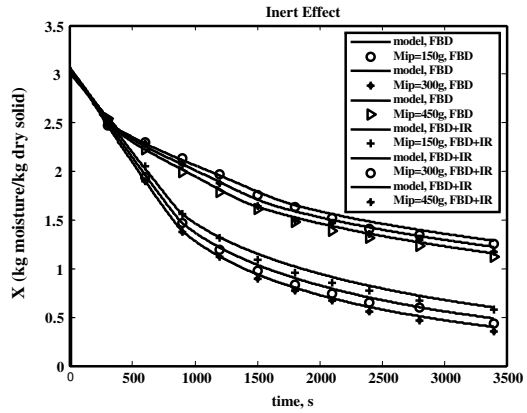

Fig. 11: Experimental and predicted average moisture contents of green peas in three different amounts of inert particle 150, 300 and 400 g in both systems (FBD & FBD+IR).

obtained by the proposed mathematical model, confirm that the chosen concepts were properly applied in developing the model. To be more specific, from this study it can be concluded that at low intensity IR, no damage is observed at the surface of the sample. This conclusion is based on the observation of the color of the surface of the sample before and after drying. At low IR intensity the advantage of surface damage was eliminated but the drying rate was increased. This is due to the fact that contrary to the conventional method, IR penetrates a few millimeters inside of the sample and causes the water to be removed by evaporation without increasing the temperature, and this effect obviously terminates at low moisture level.

Nomenclature

a_w	Water activity coefficient
A	Area, m^2
C_p	Heat capacity, kj/kg °C
D_{eff}	Effective diffusivity, m^2/s
d_{pen}	Penetration depth, m
$F_{gp\text{-}ir}$	Shape factor
h_t	Heat transfer coefficient, W/m^2 °C
h_{fg}	Heat of vaporization, kj/kg
k	Extinction coefficient, m^{-1}
K_P	Thermal conductivity, W/m °C
K_m	Mass transfer coefficient, kg/m^2s
Le	Lewis number
n	Node number
Nu	Nusselt number
Q_{Abs}	Absorption heat, W
Q_r	Relative heat, W/m^3
r	radius, m
Re	Reynolds number
R	Radius, m
Rh	Relative humidity
t	Ttime, s
T	Temperature, k
T_e	Emitter temperature, K
X	Moisture content, kg moisture/kg dry solid
y	Moisture composition at vapor phase

Greek symbols

ρ	Density, kg/m^3
σ	Boltzmann constant, $W/m^2\ k^4$
ε	Emissivity

Subscripts:

a	Air
avg	Average
e	Equilibrium
gp	Green pea
IR	Infrared
p	Particle
C	Conduction zone
p	Penetration zone
S	Surface
t	Total
∞	Bulk condition
0	Initial

Acknowledgements

The authors would like to thank the Iran National Science Foundation (INSF) and Marvdasht Islamic Azad University, Shiraz, Iran for the award of a research grant to conduct this study.

Received : Nov. 19, 2010 ; Accepted : Jan. 9, 2012

REFERENCES

[1] Panda R.C., Rao V.S.R., Fluidized Bed Dryers: Dynamic Modeling and Control, *Chem. Eng. Technol.*, **14**, p. 307 (1991).

[2] Hovmand S. Fluidized Bed Drying, In: A. S. Mujumdar (ED). "Handbook of Industrial Drying", Marcel Dekker. New York. pp 195-248, (1995).

[3] Zhou S.J., Mowla D., Wang F.R., Rudolph V., "Experimental Investigation of Good Drying Processes in Dense Phase Fluidized Bed with Energy Carrier", CHEMECA 98, Port Doulas. North Queenslands, Australia, (1998).

[4] Hatamipour M.S., Mowla D., Experimental and Theoretical Investigation of Drying of Carrots in a Fluidized Bed with Energy Carrier, *Drying Technology,* **21**(1), p. 83 (2003).

[5] Izadifar M., Mowla D., Simulation of a Cross-Flow Continuous Fluidized Bed Dryer for Paddy Rice, *Journal of Food Engineering*, **58**, p. 325 (2003).

[6] Hebbar H.U., Vishwanathan K.H, Ramesh M.N., Development of Combined Infrared and Hot Air Dryer for Vegetables, *Journal of Food Eng*., **65**, p. 557 (2004).

[7] Sandu, C., Infrared Radiative Drying in Food Engineering A Process Analysis. *Biotechnol Prog,* **2**(3), p. 159, (1986).

[8] Souraki, B. A. and Mowla, D., Experimental and Theoretical Investigation of Drying Behavior of Garlic in an Inert Medium Fluidized Bed Assisted by Microwave, *Journal of Food Engineering*. **88**, p. 438, (2008).

[9] Sakai, N., & Hanzawa, T. Applications and Advances in Far - Infrared Heating in Japan, *Trends in Food Science & Technology.* **5,** p. 357, (1994).

[10] Ginzburg, A. S. "Application of Infrared Radiation in Food Processing" Leonard Hill Books. London. pp 7-57, (1969).

[11] Afzal, M. T., Abe, T. and Hilida, Y. Energy and Quality Aspect During Combined FIR-Convection Drying of Barley, *J. Food. Eng.* , 42, p. 177 (1999).

[12] Senadeera, W. "Comparison of the Effects of Fixed Bed and Fluidized Bed Drying on Physical Properties Change of Spherical Food Material Using Peas as a Model mMaterial. Proceedings 2nd International Conference on ICFPTE`04. Asian Institute of Technology, Bankok. Pages pp. 288-296, (2004).

[13] Nindo, C. I., Kudo, Y., Bekki, E. Test Model for Studying Sun Drying of Rough Rice Using Far-Infrared Radiation. *Drying Technology-An International Journal,* **13**(1-2), p. 225, (1995).

[14] Jumah, R., Modeling and Simulation of Continuous and Intermittent Radio Frequency-Assisted Fluidized Bed Drying of Grains. *Trans IchemE, part C, Food and Bioproducts processing*, **83**(C3), p. 203, (2005).

[15] Krokida, M. K., Karathanos, V. T., Maroulis, Z. B., Marinos-Kouris, D., Drying Kinetics of Some Vegetables. *Journal of Food Engineering,* p. 391, (2003).

[16] Strumillo, C. and Kudra T., "Drying Principles, Applications, and Design", Gordon &Breach Science Publishers, USA. (1996)

[17] Chen, X.D., "Lewis Number in the Context of Air-Drying of Hygroscopic Materials" *Separation and Purification Technology*, **48** (2), p. 121 Pergamon, UK, (2006).

[18] Earle , R.L.,"Unit Operations in Food Processing" Second Edition, Pergamon Press, Oxford. (2004)

[19] Weissteins, E. "World of Physics, Lamberts Law" Available from http;//scienceworld.wolfram.com/Physics. Lamberts Law, html. (2005).

[20] Jun, S., Irudayaraj, J. Selective far Infrared Heating –Design and Evaluation. (Part I). *Drying Technology.* **21** (1), p. 51 (2003).

[21] Anon "Infrared Ceramic Heater" Sang Chai Meter Co., Ltd.,Thailand., Available from http://www.sangchaimeter.com, (2004).

[22] Arinze, E. A., Schoenau, G. J. and Besant, R. W. "A dynamic thermal performance simulation model of an energy conserving greenhouse with thermal storage". ASAE Paper No. 84-2702.(1984).

[23] Kunii, D., Levenspiel ,O., "Fluidization Engineering" 2nd edition, Butterworth-Heinemann, Stoneham, MA, USA, (1991).

[24] Ghisalberti, L., Kondjoyan, A. Convective Heat Transfer Coefficient Between Air Flow and a Short Cylinder. Effect of Air Velocity and Turbulence. Effect of Body Shape, Dimensions and Position in the Flow. *Journal of Food Eng*. **42** , p. 33 (1999).

[25] Botterill, J. S. M., "Fluid Bed Heat Transfer" Academic Press, London pp 145-228, (1975).

[26] Incropera, F. P., Dewitt, D. P., "Fundamental of Heat and Mass Transfer" New York, John Wiley and Sons. Pp325-465, (1996).

[27] Pakowski, Z., Bartczak, Z., Strumilo, C., & Stenstrom, S. Evaluation of Equations Approximating Thermodynamic and Transport Properties of Water, Steam and Air for Use in CAD of Drying Processes, *Drying Technology- An International Journal,* **9**(3), p. 753, (1991).

[28] Honarvar, B., Mowla, D., Safekordi, A. A. Experimental and Theoritical Investigation of Drying of a Cylindrical Particle in a Fluidized Bed Dryer of Energy Carrier particles by Hot air and Infrared Radiation Sources. *Iran. J. Chem. Chem Eng. (IJCCE)* **28**(4) , p. 41, (2009).

[29] Mowla, D., Honarvar, B., Safekordi, A. A., Soltanieh, M., Bastani, D., Experimental Study of Physical Properties of a Potato in a Fluidized Bed Dryer of Inert Particles Assisted by Infrared Heat Soyrces, *Iran. J. Chem. Chem. Eng. (IJCCE),* **29**(1), p. 81, (2010).